Superhydrophobic surfaces via controlling the morphology of ZnO micro/nano complex structure*

Gong Mao-Gang(公茂刚)†, Xu Xiao-Liang(许小亮)‡, Yang Zhou(杨 周), Liu Yan-Song(刘艳松), and Liu Ling(刘 玲)

Department of Physics, University of Science and Technology of China, Hefei 230026, *China*

(Received 28 October 2009; revised manuscript received 23 November 2009)

ZnO micro/nano complex structure films, including reticulate papillary nodes, petal-like and flake-hole, have been self-assembled by a hydrothermal technique at different temperatures without metal catalysts. The wettability of the above film surfaces was modified with a simple coating of heptadecafluorodecyltrimethoxy-silane in toluene. After modifying, the surface of ZnO film grown at 50 °C was converted from superhydrophilic with a water contact angle lower than 5° to superhydrophobic with a water contact angle of 165°. Additionally, the surface of reticulate papillary nodes ZnO film grown at 100 °C had excellent superhydrophobicity, with a water contact angle of 173° and a sliding angle lower than 2°. Furthermore, the water contact angle on the surface of petal-like and flake-hole ZnO films grown at 150 °C and 200 °C were found to be 140° and 120°, respectively. The wettability for the samples was found to depend strongly on the surface morphology which results from the growth temperature.

Keywords: hydrothermal, superhydrophobic, ZnO, micro/nano complex structure
PACC: 6770, 6855, 8116D

1. Introduction

A self-cleaning phenomenon has been found in nature, such as in the Lotus effect and on water strider legs.[1] There have been many attempts to produce materials with similar water-repelling properties synthetically, employing methods such as chemical vapour deposition,[2] sol-gels,[3] plasma etching,[4] template growth,[5] chemical deposition,[6] and layer-by-layer deposition.[7]

Modifying the surface wettability of semiconductor surfaces would be valuable in many situations. Given the relative simplicity of fabricating one-dimensional (1D) nanostructures, ZnO has shown a great potential for use in next-generation nano devices.[8] Field-effect transistors, room-temperature UV nano-lasers, piezoelectric nano-generators, light-emitting diodes, and UV photo-detector based on ZnO nanorods or nanowires have been reported.[9−14] Recently, microtextured ZnO surfaces have been introduced to create superhydrophobic surfaces via chemo- or electro-deposition.[15−17]

In the following text, we will introduce a hydrothermal method to facilitate the fabrication of large-scale reticulate papillary nodes, petal-like and flake-hole ZnO films at low temperature with good controllability and reproducibility. The fabrication of the superhydrophobic ZnO surface was composed of three steps. First, the ZnO seed layer was deposited on the Si substrates by r.f. magnetron sputtering. Next, the ZnO micro/nano complex structure was formed by chemical reaction in a mixed aqueous solution of zinc acetate dehydrate and hexamethylene tetramine. Finally, the as-prepared micro/nano complex structure was modified by heptadecafluorodecyltrimethoxy-silane (HTMS) coating to obtain a superhydrophobic surface. The superhydrophobic properties of different samples were depicted by the water contact angle (WCA) and sliding angle (SA). The goal was to create surfaces with high WCA and small SA which induce the formation of water droplets that roll away and remove dirty particles on the ZnO surface.[18]

2. Experimental

2.1. Preparation of samples

The pressed ZnO powder (99.99%) target prepared for r.f. magnetron sputtering was calcined in a Muffle at 1200° for 5h in ambient air, and was then

*Project supported by the 973 Program of China (Grant No. 2006CB302900) and National Natural Science Foundation of China (Grant No. 50872129).
†E-mail: gmg@mail.ustc.edu.cn
‡Corresponding author. E-mail: xlxu@ustc.edu.cn
© 2010 Chinese Physical Society and IOP Publishing Ltd

naturally cooled to room temperature. The chemical reagents, such as zinc acetate dehydrate (Zn-AD, purity 99.0+%), hexamethylene tetramine (He-T, purity 99.0+%), ethanol (purity 99.7+%), acetone (purity 99.7+%) and n-Toluene (purity 97+%) were obtained from Sinopharm Chemical Reagent Co., Ltd, China and used without further purification. The resistivity of the deionized water was 18.25 (MΩ·cm).

The Si(111) substrates were first immersed in the boiling 98% H_2SO_4 for 10 min, then ultrasonically washed with acetone, ethanol and deionized water, respectively, and finally dried in a far infrared drying oven. The 10 nm ZnO seed layer was then deposited on the Si substrates by r.f. magnetron sputtering. The background pressure of the vacuum chamber was 1×10^{-4} Pa. A mixture of oxygen and argon with a volume ratio of 1:1 was used as the sputtering gas with a total pressure of 3 Pa. The ZnO seeds were annealed in air for 1 h at 550 °C to remove the interstitial Zn. After this was done, the ZnO micro/nano complex structure was grown.

Each of the first set of the samples was prepared by immersing the substrates vertically in the mixed 0.01 mol/L Zn-AD and 0.01 mol/L He-T aqueous solution for 2, 4, 6 or 12 hours. This vertical strategy had two benefits. First, the nanowires' growth depended mainly on the adsorption of ZnO nuclei in the reaction solution and avoided the ZnO nuclei deposition that forms easily in the spaces among nanowires. Secondly, this also largely precluded the possibility of simple precipitation contributing to materials on the substrate surface.[19] The reaction temperature for these growths was kept at 100 °C. The as-grown ZnO nanowires film showed up as well-aligned dispersed ZnO nanowires.[20] After immersion in deionized water for just 10 seconds, these samples were dried in a far infrared oven at 80 °C for 5 min. Results show that the ZnO nanowires assembled into reticulate papillary nodes structure via surface tension of the water.[21]

The second set of the samples were prepared by immersing the substrates vertically in the mixed 0.01 mol/L Zn-AD and 0.01 mol/L He-T aqueous solution. The reaction time was kept for 12 h. In order to test the temperature effect on the configuration of the ZnO micro/nano structures, the reaction temperature was varied among the following temperatures 50 °C, 100 °C, 150 °C and 200 °C. The rest of the process was the same as that for the first set of the samples.

The resulting ZnO thin films were immersed in the modification solution (2 parts HTMS mixed with 98 parts absolute toluene by volume) for 12 h to obtain the lower energy surface. The reaction conditions, the WCA and SA for all samples are summarized in Table 1 as follows.

Table 1. Summarized reaction conditions, water contact angle and sliding angle.

samples	growth time/h (T=100°)	2	4	6	12
1st set	WCA	173°	172°	170°	169°
	SA	1°	1°	2°	2°
	nanowires density/($\times10^9$/cm^2)	1.3	1.5	1.8	2.3
samples	reaction temperature/(°) (t=12 h)	50	100	150	200
2nd set	WCA	165°	169°	140°	120°
	SA	5°	2°	$>90°$	$>90°$

Note: nanowires' density error is $\pm0.1\times10^9$/cm^2, errors for the WCA and SA are ±1°.

2.2. Surface characterization

The morphology of the ZnO samples was revealed by field emission scanning electron microscopy (FESEM). The WCA and SA were measured by the CAST2.0 contact angle analysis system (Solon Information Technology Co. Ltd., Shanghai) at ambient temperature. Droplets of liquids with a volume of 8 μL were used to measure the WCA. The SA was measured by tilting the stage and recording the point at which the droplet began to roll downhill. Each WCA measurement was repeated five times at different places on the sample, and the mean value was reported.

3. Results and discussion

3.1. Characterization of ZnO micro/nano complex structure

Figure 1 shows the FESEM images of the reticulate papillary nodes ZnO nanowires (1st set of the samples). Figures 1(a), 1(b), 1(c) and 1(d) correspond to growth times of 2 h, 4 h, 6 h, and 12 h, respectively. All the ZnO nanowires have hexagonal wurtzite structure. The diameter of the reticulate ZnO nanowires (from 20 nm to 60 nm, with an average of 42 nm) almost shows no obvious change with increasing growth time. The average density of the ZnO nanowires, however, increased from 1.3×10^9 cm^{-2} grown for 2 h to 2.3×10^9 cm^{-2} grown for 12 h. The increase of the nanowires density can be attributed to more and more nano-seeds growing into nanowires as process time increased. The growth mechanism of the reticular papillary nodes structure could be attributed to the water's surface tension, the horizontal component of which is large enough to make the top of several ZnO nanowires congregate from the flash evaporation of the water (in the far infrared drying oven at 80 °C).[21] Another requirement for forming such structures is that the diameter of the ZnO nanowires is sufficiently small and the aspect ratio is sufficiently large. The relationship between the reticular papillary nodes structure and hydrophobicity will be discussed in the following section.

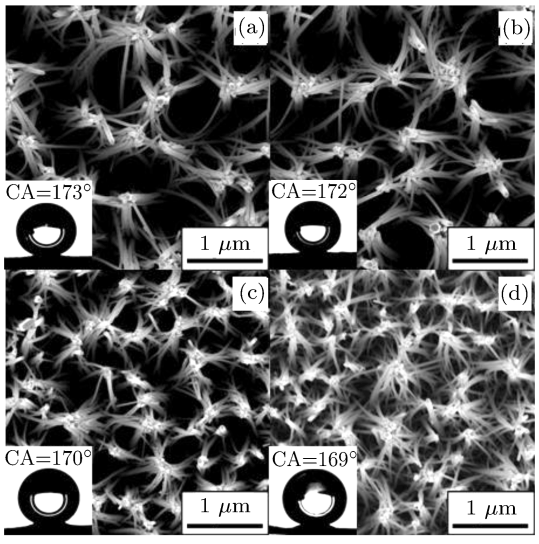


Fig. 1. FESEM images of the reticulate papillary nodes ZnO nanowires with growth times of (a) 2 h, (b) 4 h, (c) 6 h, and (d) 12 h. The insets are optical images of water droplets on the sample surface with a coating of HTMS, during the contact angle measurement.

Figure 2 shows the FESEM images of the second set of samples, where the initial reagents concentration of both Zn-AD and He-T were 0.01 mol/L. Figure 2(a) shows that ZnO nanowires grown at 50 °C for 12 h aggregated into the reticulate papillary node structure, after drying in the far infrared drying oven at 80 °C for 5 min. When the reaction was performed at 100° for 12 h, the shape of ZnO also changed from dispersed nanowires to reticulate papillary nodes after the same drying process (see Fig. 2(b)). Regarding the surface morphology shown in Figs.2(a) and 2(b), the resulting surface exhibits a special reticulate structure, which is rough enough to trap air, and along with the low surface free energy, leads to superhydrophobicity. When maintaining the reaction conditions for preparing ZnO nanowires but increasing temperature to 150 °C, petal-like ZnO formed and distributed very evenly across the whole substrate (see Fig. 2(c)). As the temperature increased to 200 °C, the petal-like ZnO structures with strong adsorption to the substrate were gradually replaced by the sparse flake-hole ZnO (see Fig. 2(d)).

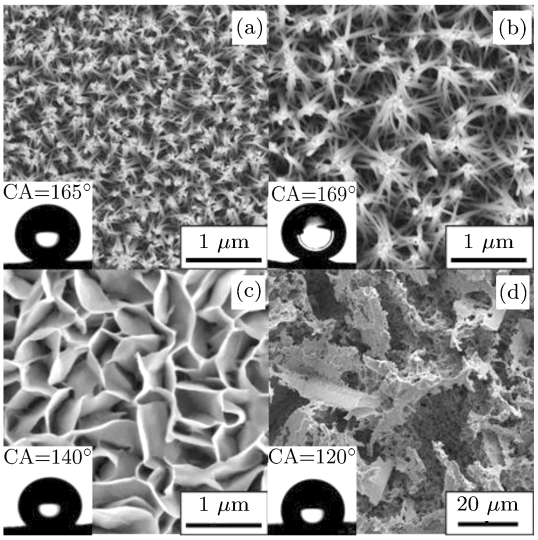


Fig. 2. FESEM images of ZnO micron/nano-structures at growth temperatures of (a) 50 °C, (b) 100 °C, (c) 150 °C and (d) 200 °C; the insets are optical images of water droplets on the sample surface with a coating of HTMS, during the contact angle measurement.

3.2. Hydrophobic and hysteresis behaviour

Wetting behaviour on a solid surface can be explained by the Wenzel[22] and Cassie[23] models. The Wenzel equation relates the rough and smooth surfaces using the roughness factor, r, which is given by

$$\cos\theta_{\rm e} = r\cos\theta_0, \tag{1}$$

where θ_e and θ_0 correspond to equilibrium WCA of the inhomogeneous and flat solid surface, respectively. r is defined as the ratio between the actual surface area and the projected surface area of the rough surface. This equation is valid only for moderate values of r when $-1 \leq r\cos\theta_0 \leq 1$.

The Cassie–Baxter model is an extension of the Wenzel model for a composite liquid–solid–air interface. In contrast to the Wenzel model, the Cassie–Baxter model predicts that a liquid–solid–air composite may form with air pockets trapped in the valleys between asperities for a rough surface. This is given by

$$\cos\theta_e = f\cos\theta_0 - (1-f), \tag{2}$$

where f is the area fraction of the protruded areas. Equation (2) has been recently modified to account for the local surface roughness on the wetted area as follows[24,25]

$$\cos\theta_e = r_e f\cos\theta_0 - (1-f), \tag{3}$$

where f is the fraction of the projected area of the solid surface wetted by water and r_e is the surface roughness of the wetted area. For the surface mainly composed of HTMS ($\theta_0 = 114°$ for a smooth ZnO surface coating with HTMS), the $r_e > 1$ for a rough surface, which, in comparison with a smooth wetted area, can enhance the surface hydrophobicity. Clearly, the prepared films mainly composed of HTMS with the special micro/nano complex structure will have even higher values of r_e. Once roughness r_e reaches a certain level, air may become trapped underneath water droplets within the interstices of the micro/nano complex structures, which would further enhance the surface hydrophobicity and lead to superhydrophobicity. This may be used to explain the WCA value in Fig. 3.

Figure 3(a) shows the WCA values on the surface of the first set of samples. According to the Cassie model, the trapped air among reticulate papillary nodes would increase the liquid–air contact area, thereby formed bigger WCA. As the growth time was increased from 2 h to 6 h, the density of ZnO nanowires increased as more and more ZnO seeds grew to nanowires, and the spacing between papillary nodes decreased gradually (Fig. 1). Meanwhile, the WCA decreased from 173° to 170° and SA increased from 1° to 2°. When the growth time reached 12 h, the WCA and SA became 169° and 2°, just a little change from the 6 h sample. This is all in accordance with the Cassie model, in that the more the air area fraction, the greater the WCA.

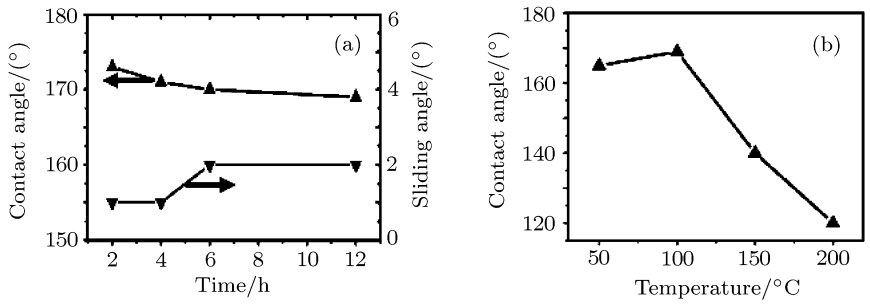


Fig. 3. Contact and sliding angles on the surface of ZnO films grown at different (a) time, and (b) temperature (in which the data of sliding angle neglected).

Figure 3(b) shows the WCA value on the surface of the second set samples. The final morphology of ZnO nanowires grown at 50 °C is similar to that of nanowires grown at 100 °C (see Figs. 2(a) and 2(b)). However, the WCA on the surface of ZnO films (50 °C, 165°) is smaller than that of the latter (100 °C, 169°). This could be attributed to the degree of ZnO nanowires congregation. The aspect ratio of ZnO nanowires grown at 50 °C (41:1) is smaller than that of the latter (104:1). When the horizontal component of water's surface tension reaches a certain value, the degree of assembly increases as the aspect ratio of nanowires increases. In the case of very large degree of assembly, larger interstices were formed among reticulate papillary nodes of ZnO nanowires. Thus, we know from the Cassie model that the superhydrophobicity of the ZnO film growth at 50 °C should be a little poorer than that of ZnO film growth at 100 °C.

When $T = 150$ °C, the surface of the sample became petal-like with low roughness (Fig. 2(c)). It also had a somewhat large WCA of 140°, but the SA exceeded 90°. The surface adhesion strength was too great to be suitable for self-cleaning. When $T = 200$ °C, the reaction resulted in a flake-hole structure (see Fig. 2(d)). The space among the flake was too big to hold up the water droplet, causing the WCA to decrease to 120° but the SA to exceed 90°.

To sum up, the reticulate papillary nodes structure grown at 100 °C followed the superhydrophobic Cassie's model more than other samples, being best in demonstrating self-cleaning morphology.

3.3. The formation mechanism of the micro/nano complex structure ZnO and the modification process

In the hydrothermal conditions, the growth of micro/nano complex structure ZnO underwent three processes: 1) hexamethylene tetramine in water solution hydrolysised to generate NH_4^+ and OH^-. 2) Zn^{2+} in the mixed solution and OH^- reacted to generate $Zn(OH)_2$. 3) $Zn(OH)_2$ continued hydrolysis to generate a certain structure of ZnO nuclei. The ZnO seeds (grown by r.f. magnetron sputtering) on the substrate grew as targets to adsorb the ZnO nuclei, forming the wires, petal-like or flake-hole ZnO. The different reaction conditions resulted in different structures (see Figs. 1 and 2). Hydrothermal reaction equations are listed as follows:

$$(CH_2)_6N_4 + 6H_2O = 6HCOH + 4NH_3$$
$$NH_3 + H_2O = NH_4^+ + OH^-$$
$$Zn_2^+ + 2OH^- = Zn(OH)_2$$
$$Zn(OH)_2 = ZnO + H_2O.$$

It is well known that two conditions are necessary to form a superhydrophobic surface: a sufficiently rough structure and low surface energy. In general, some organic modification is needed to obtain a low surface energy. The HTMS solution modification process is shown by Fig. 4. The as-grown ZnO films usually carry many hydrophilic OH groups from exposure to the atmosphere. The HTMS also hydrolyzed with the OH to generate methanol. As a result, many long C–F chains formed on the surface of ZnO films. The new-born chains with CF_2 and CF_3 groups significantly decreased the surface free energy. Combining the roughness and low free energy, the modified micro/nano complex structure ZnO surface showed a dramatic increase in air trapping, which made the surface of ZnO film superhydrophobic with high WCA and low SA.

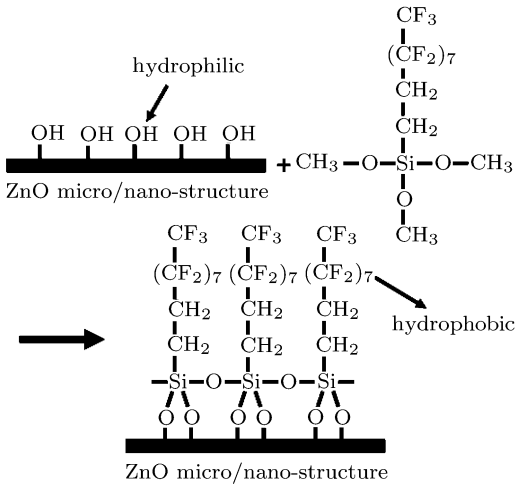


Fig. 4. Modification mechanism of the micro/nano complex structure ZnO surface using HTMS solution.

4. Conclusion

In summary, micro/nano complex structure ZnO with a range of well-defined morphologies, such as reticulate papillary nodes nanowires, petal-like and flake-hole structures have been fabricated by an aqueous solution approach. From the results, the temperature impact on the morphology appears to be greater than the growth time. All the samples were transformed from hydrophilic to hydrophobic, and sometimes even superhydrophobic after being modified by the HTMS in toluene. The superhydrophobic function of the ZnO film surface will greatly extend the service life of the ZnO based micro/nano devices and expand the fields of application of the ZnO materials.

References

[1] Barthlott W and Neinhaus C 1997 *Planta* **202** 1

[2] Liu H, Feng L, Zhai J, Jiang L and Zhu D B 2004 *Langmuir* **20** 5659

[3] Ebril H Y, Demirel A L, Avci Y and Mert O 2003 *Science* (Washington, D C, U.S.) **299** 1377

[4] Jin M H, Feng X J, Xi J M, Zhai J, Cho K, Feng L and Jiang L 2005 *Macromol. Rapid Commun.* **26** 1805

[5] Li J, Fu J, Cong Y, Wu Y, Xue L J and Han Y C 2006 *Appl. Surf. Sci.* **252** 2229

[6] Zhao N, Shi F, Wang Z Q and Zhang X 2005 *Langmuir* **21** 4713
[7] Han J T, Zheng Y, Cho J H, Xu X and Cho K 2005 *J. Phys. Chem.* B **109** 20773
[8] Gudiksen M S, Lauhon L J, Wang J F, Smith D C and Lieber C M 2002 *Nature* **415** 617
Cui Y and Lieber C M 2001 *Science* **291** 851
Star A, Lu Y, Bradley K and Grüner G 2004 *Nano Lett.* **4** 1587
Marty L, Bonhomme A, Iaia A, André E, Rauwel E, Dubourdieu C, Toffoli A, Ducroquet F, Bonnot A M and Bouchiat V 2006 *Nanotechnology* **17** 5038
[9] Huang M H, Mao S, Feick H, Yan H Q, Wu Y Y, Kind H, Weber E, Russo R and Yang P D 2001 *Science* **292** 1897
[10] Kim H J, Lee C H, Kim D W and Yi G C 2006 *Nanotechnology* **17** 327
Liu H X, Zhou S M, Li S Z, Hang Y, Xu J, Gu S L and Zhang R 2006 *Acta Phys. Sin.* **55** 1398 (in Chinese)
[11] Konenkamp R, Word R C and Godinez M 2005 *Nano Lett.* **5** 2005
[12] Wang Z L and Song J H 2006 *Science* **312** 242
[13] Soci C, Zhang A, Xiang B, Dayeh S A, Aplin D P R, Park J, Bao X Y, Lo Y H and Wang D 2007 *Nano Lett.* **7** 1003
[14] Wang J X, Sun X W, Yang Y, Huang H, Lee Y C, Tan O K and Vayssieres L 2006 *Nanotechnology* **17** 4995
[15] Li M, Zhai J, Liu H, Song Y, Jiang L and Zhu D 2003 *J. Phys. Chem.* B **107** 9954
Ma K, Li H, Zhang H, Xu X L, Gong M G and Yang Z 2009 *Chin. Phys.* B **18** 1942
[16] Zhang X, Sato O and Fujishima A 2004 *Langmuir* **20** 6065
[17] Liu H, Feng L, Zhai J, Jiang L and Zhu D 2004 *Langmuir* **20** 5659
[18] Chiou N R, Lu C M, Guan J J, Lee L J and Epstein A J 2007 *Nature Nanotechnology* **2** 354
[19] Gong M G, Xu X L, Cao Z L, Liu Y Y and Zhu H M 2009 *Acta Phys. Sin.* **58** 1885 (in Chinese)
[20] Guo M, Diao P and Cai S M 2007 *Thin Solid Films* **515** 7162
[21] Gong M G, Xu X L, Yang Z, Liu Y Y, Lv H F and Lv L 2009 *Nanotechnology* **20** 165602
[22] Wenzel R N 1936 *Ind. Eng. Chem.* **28** 988
[23] Cassie A B D and Baxter S 1944 *Trans. Faraday Soc.* **40** 546
[24] Marmur A 2003 *Langmuir* **19** 8343
[25] Michielsen s and Lee H J 2007 *Langmuir* **23** 6004